

Supporting Information

for paper

Synthesis, structural features, magnetic properties and thermal decomposition of a new series of polymeric Ln(III)-Cr(III) cyclopropane-1,1-dicarboxylates

Evgeniya S. Bazhina^{a,*}, Maxim A. Shmelev^a, Julia K. Voronina^a, Natalia A. Korotkova^a, Konstantin A. Babeshkin^a, Anna K. Matiukhina^a, Ekaterina V. Belova^b, Natalia V. Gogoleva^a, Sergey Yu. Kottsov^a, Nikolay N. Efimov^a, Mikhail A. Kiskin^a, and Igor L. Eremenko^a

^a *N.S. Kurnakov Institute of General and Inorganic Chemistry of the Russian Academy of Sciences, Leninsky prosp. 31, Moscow 119991, Russian Federation*

E-mail: evgenia-VO@mail.ru

^b *M.V. Lomonosov Moscow State University, Department of Chemistry, Leninskie Gory 1/3, 119991 Moscow, Russian Federation*

I. X-ray powder diffraction patterns

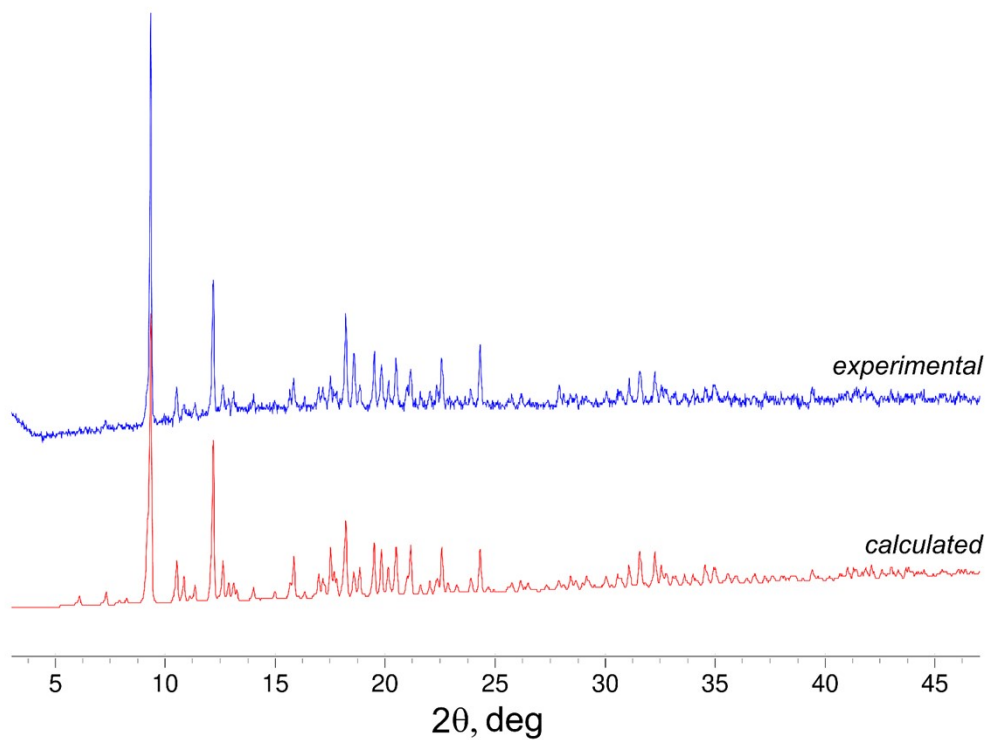


Fig. S1. The experimental PXRD pattern for 1_{Eu} measured at 295 K and its comparison with calculated data for 1_{Eu} .

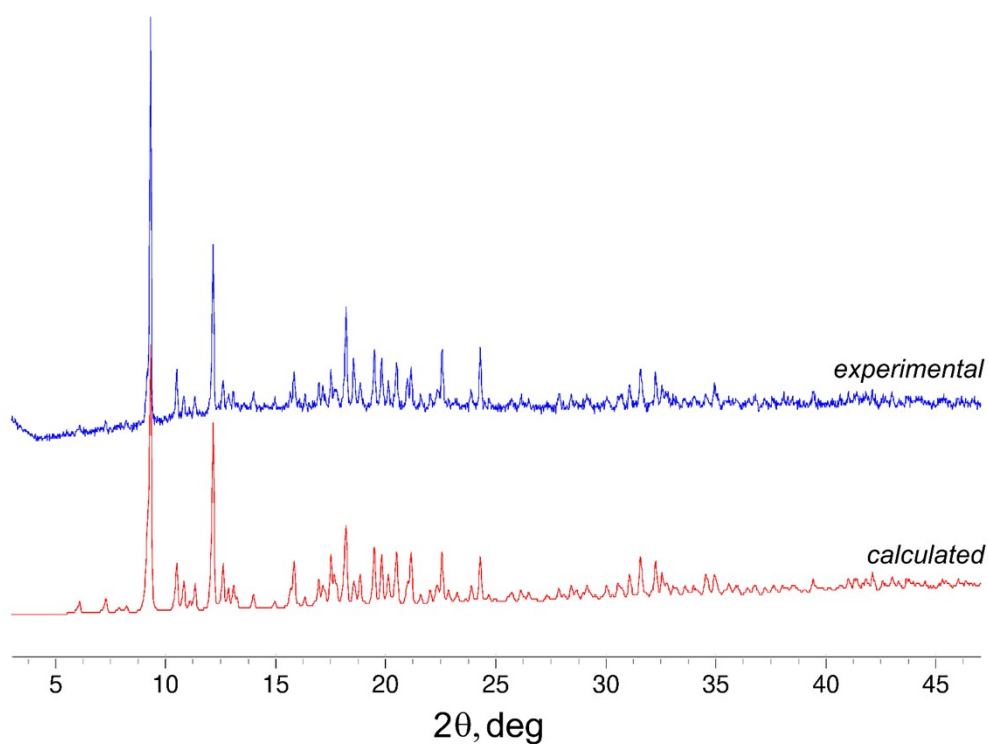


Fig. S2. The experimental PXRD pattern for 1_{Gd} measured at 295 K and its comparison with calculated data for 1_{Gd} .

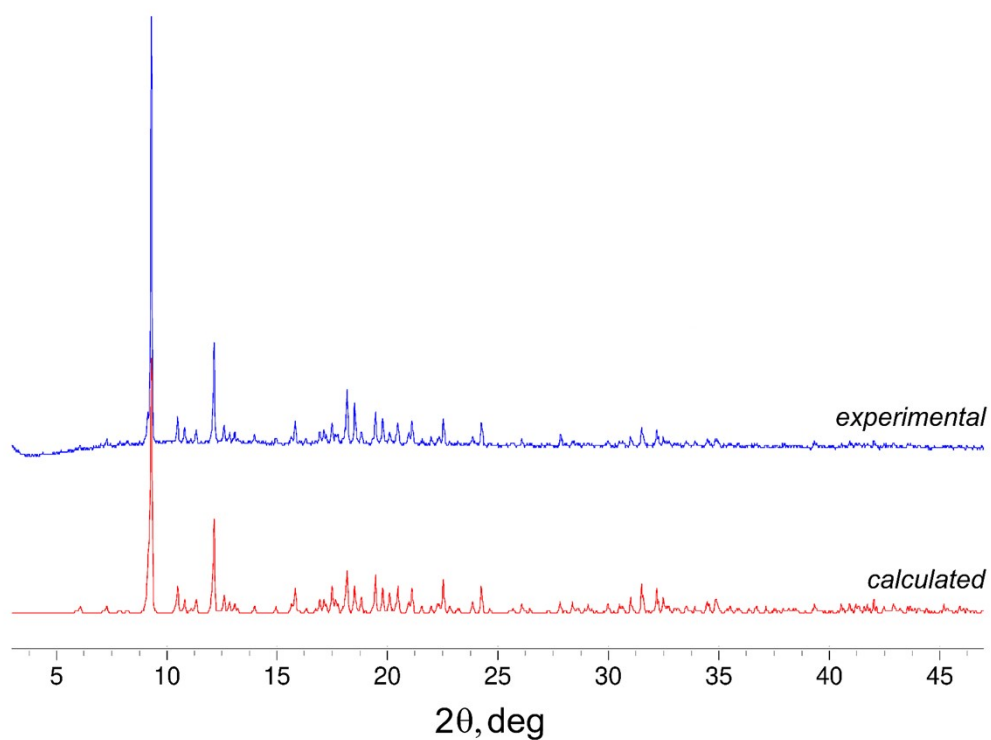


Fig. S3. The experimental PXR D pattern for 1_{Tb} measured at 295 K and its comparison with calculated data for 1_{Tb} .

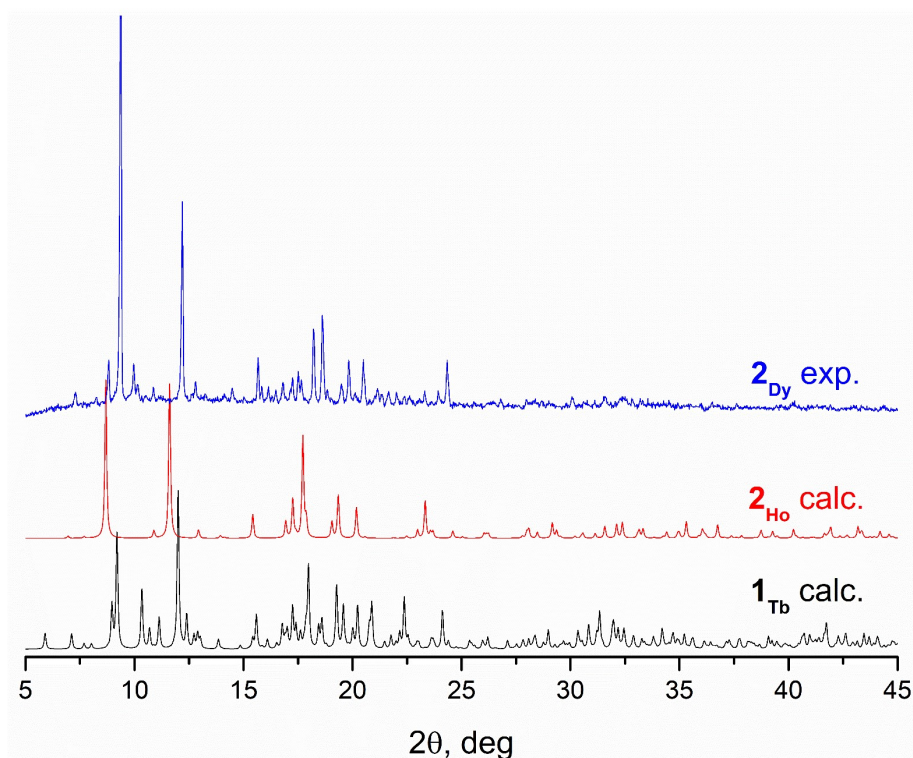


Fig. S4. The experimental PXR D pattern for 2_{Dy} measured at 295 K and its comparison with data calculated from single-crystal XRD for 1_{Tb} and 2_{Ho} .

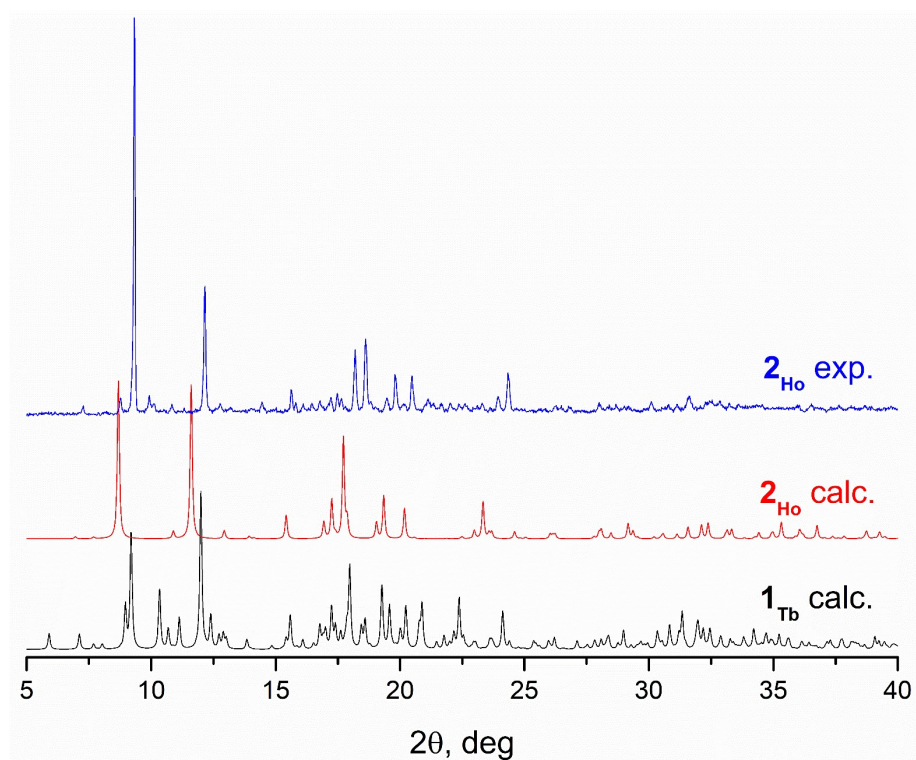


Fig. S5. The experimental powder XRD pattern for **2_{Ho}** measured at 295 K and its comparison with data calculated from single-crystal XRD for **1_{Tb}** and **2_{Ho}**.

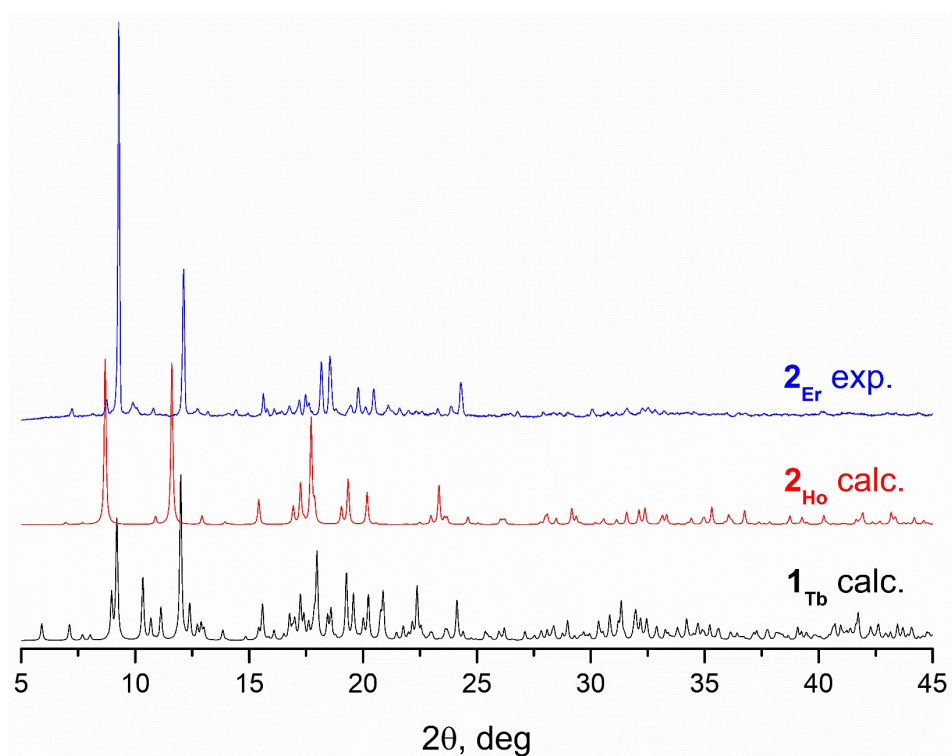


Fig. S6. The experimental powder XRD pattern for **2_{Er}** measured at 295 K and its comparison with data calculated from single-crystal XRD for **1_{Tb}** and **2_{Ho}**.

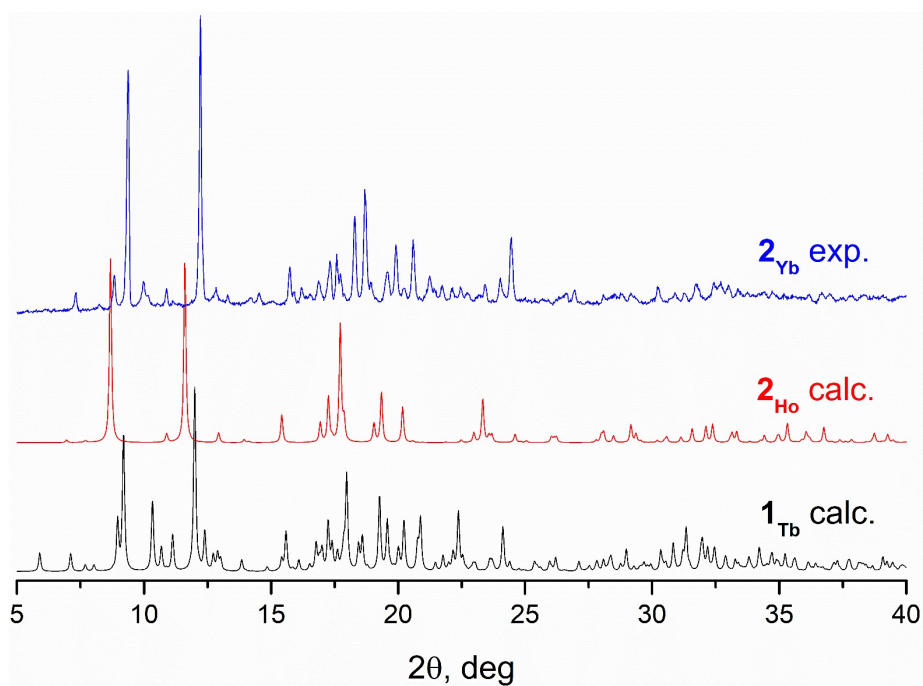


Fig. S7. The experimental powder XRD pattern for 2_{Yb} measured at 295 K and its comparison with data calculated from single-crystal XRD for 1_{Tb} and 2_{Ho} .

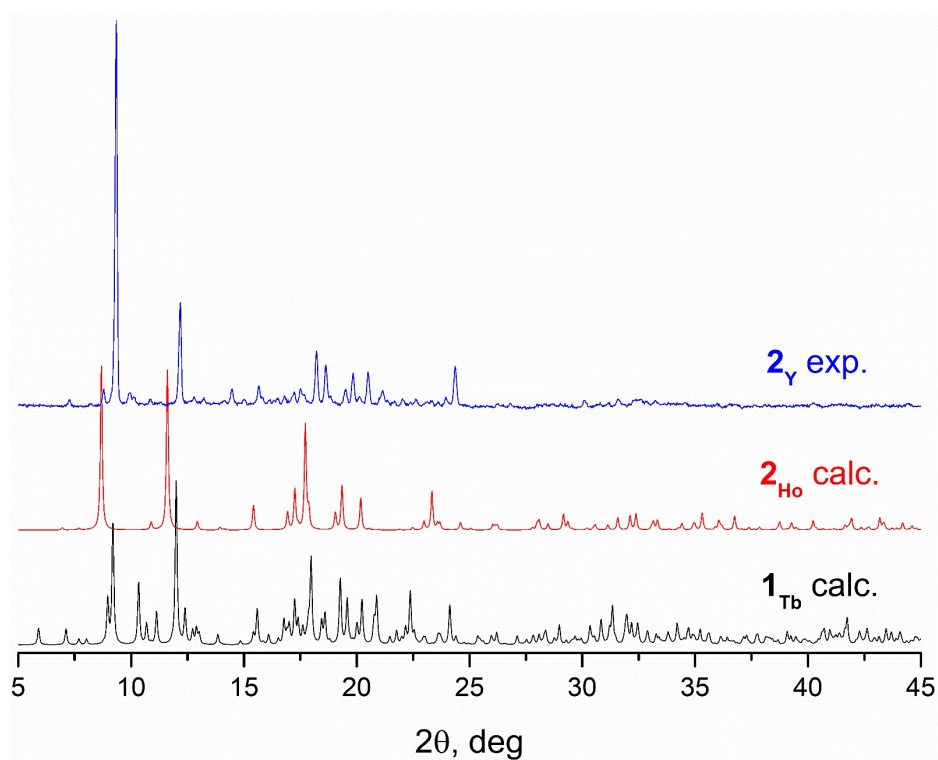


Fig. S8. The experimental powder XRD pattern for 2_Y measured at 295 K and its comparison with data calculated from single-crystal XRD for 1_{Tb} and 2_{Ho} .

II. The description of crystal structures

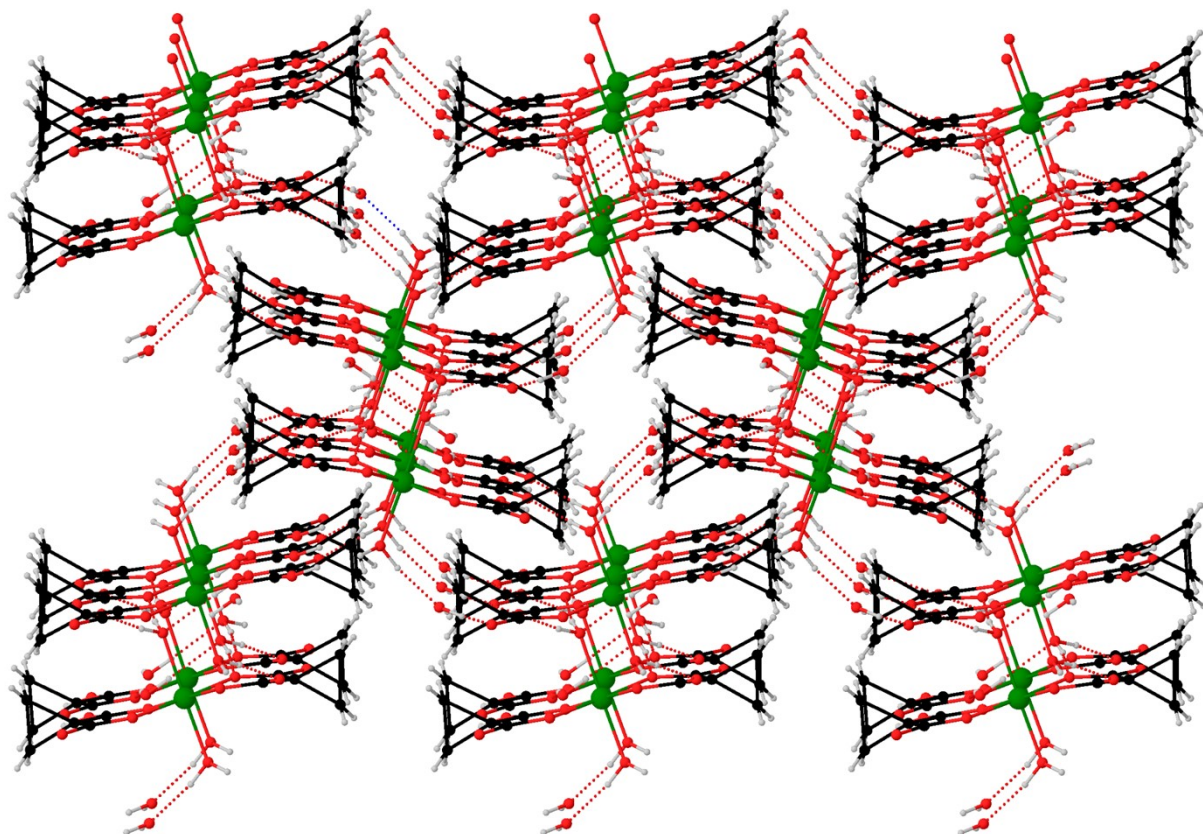


Fig. S9. The fragment of crystal packing of compound 3.

Table S1. Continuous shape measures (CShM) for LnO₈ coordination polyhedra in compounds **1_{Eu}**, **1_{Gd}**, **1_{Tb}**. The lowest SHAPE values are shown highlighted indicating best fits.

Structure, Ln	SAPR-8	TDD-8	JBTPR-8	BTPR-8	JSD-8
1_{Eu}, Eu1	2.378	1.149	1.627	0.952	3.224
1_{Eu}, Eu2	0.773	1.040	1.890	1.325	3.488
1_{Gd}, Gd1	2.290	1.099	1.655	0.948	3.261
1_{Gd}, Gd2	0.761	1.076	1.860	1.313	3.499
1_{Tb}, Tb1	2.238	1.126	1.674	0.955	3.359
1_{Tb}, Tb2	0.670	1.151	1.877	1.336	3.558

Codes:

SAPR-8 (D_{4d}) Square antiprism;

TDD-8 (D_{2d}) Triangular dodecahedron;

JBTPR-8 (C_{2v}) Biaugmented trigonal prism J50;

BTPR-8 (C_{2v}) Biaugmented trigonal prism;

JSD-8 (D_{2d}) Snub diphenoid J84.

Table S2. Selected bond angles ω (deg.) for 1_{Eu} .

Angle	ω	Angle	ω
O7A–Eu1–O11A ⁽ⁱ⁾	87.63(12)	O3A–Eu2–O8A ⁽ⁱ⁾	73.01(12)
O7A–Eu1–O1	73.73(12)	O3A–Eu2–O3B	74.76(12)
O7A–Eu1–O2	80.84(12)	O3A–Eu2–O12B ⁽ⁱⁱⁱ⁾	111.71(12)
O7A–Eu1–O3	143.51(11)	O3A–Eu2–O6	74.81(12)
O7A–Eu1–O4	87.53(12)	O3A–Eu2–O7	142.23(12)
O7A–Eu1–O5	74.01(11)	O3A–Eu2–O8	143.30(13)
O11Ai–Eu1–O5	69.74(13)	O3A–Eu2–O9	85.70(13)
O11B ⁽ⁱⁱ⁾ –Eu1–O7A	146.20(12)	O8A ⁽ⁱ⁾ –Eu2–O6	135.69(12)
O11B ⁽ⁱⁱ⁾ –Eu1–O11A ⁽ⁱ⁾	112.49(12)	O8A ⁽ⁱ⁾ –Eu2–O8	74.45(12)
O11B ⁽ⁱⁱ⁾ –Eu1–O1	73.96(12)	O8A ⁽ⁱ⁾ –Eu2–O9	79.39(12)
O11B ⁽ⁱⁱ⁾ –Eu1–O2	80.99(12)	O3B–Eu2–O8Ai	123.50(12)
O11B ⁽ⁱⁱ⁾ –Eu1–O3	69.84(12)	O3B–Eu2–O12B ⁽ⁱⁱⁱ⁾	72.53(12)
O11B ⁽ⁱⁱ⁾ –Eu1–O4	91.54(13)	O3B–Eu2–O6	74.71(13)
O11B ⁽ⁱⁱ⁾ –Eu1–O5	137.42(12)	O3B–Eu2–O8	139.23(12)
O1–Eu1–O11A ⁽ⁱ⁾	141.85(12)	O3B–Eu2–O9	141.79(12)
O1–Eu1–O5	132.09(12)	O12B ⁽ⁱⁱⁱ⁾ –Eu2–O8Ai	78.09(12)
O2–Eu1–O11A ⁽ⁱ⁾	70.38(11)	O12B ⁽ⁱⁱⁱ⁾ –Eu2–O6	143.09(13)
O2–Eu1–O1	73.91(12)	O12B ⁽ⁱⁱⁱ⁾ –Eu2–O8	77.20(12)
O2–Eu1–O3	122.32(12)	O12B ⁽ⁱⁱⁱ⁾ –Eu2–O9	145.67(12)
O2–Eu1–O5	133.18(12)	O7–Eu2–O8Ai	144.74(13)
O3–Eu1–O11A ⁽ⁱ⁾	76.49(11)	O7–Eu2–O3B	78.06(12)
O3–Eu1–O1	136.18(12)	O7–Eu2–O12B ⁽ⁱⁱⁱ⁾	83.91(13)
O3–Eu1–O5	69.70(11)	O7–Eu2–O6	73.06(13)
O4–Eu1–O11A ⁽ⁱ⁾	141.86(13)	O7–Eu2–O8	72.10(12)
O4–Eu1–O1	71.59(13)	O7–Eu2–O9	100.38(13)
O4–Eu1–O2	145.44(12)	O8–Eu2–O6	120.27(12)
O4–Eu1–O3	85.39(13)	O8–Eu2–O9	72.00(12)
O4–Eu1–O5	72.55(13)	O9–Eu2–O6	68.54(12)

Symmetry codes: (i) $x-1/2, -y+1/2, -z+1/4$; (ii) $-y+1, -x+1, -z+1/2$; (iii) $x-1/2, -y+3/2, -z+1/4$.**Table S3.** Selected bond angles ω (deg.) for 1_{Gd} .

Angle	ω	Angle	ω
O1–Gd1–O5	131.53(19)	O3A–Gd2–O3B	111.68(18)
O1–Gd1–O11A ⁽ⁱ⁾	142.03(17)	O3A–Gd2–O6	142.00(18)
O2–Gd1–O1	74.38(17)	O3A–Gd2–O7	143.20(19)
O2–Gd1–O3	146.34(19)	O3A–Gd2–O8A ⁽ⁱⁱⁱ⁾	73.01(18)
O2–Gd1–O4	122.46(18)	O3A–Gd2–O8	85.28(19)
O2–Gd1–O5	133.49(18)	O3A–Gd2–O9	74.93(17)
O2–Gd1–O11A ⁽ⁱ⁾	70.14(17)	O3A–Gd2–O12B ^(iv)	74.57(17)
O3–Gd1–O1	72.00(19)	O3B–Gd2–O7	77.57(18)
O3–Gd1–O4	84.37(19)	O3B–Gd2–O8A ⁽ⁱⁱⁱ⁾	78.04(18)
O3–Gd1–O5	71.7(2)	O3B–Gd2–O8	146.13(18)

O3–Gd1–O11A ⁽ⁱ⁾	141.42(19)	O3B–Gd2–O9	142.38(18)
O4–Gd1–O1	136.06(17)	O6–Gd2–O3B	84.3(2)
O4–Gd1–O5	69.48(17)	O6–Gd2–O7	72.25(18)
O4–Gd1–O11A ⁽ⁱ⁾	76.68(16)	O6–Gd2–O8A ⁽ⁱⁱⁱ⁾	144.98(19)
O4B–Gd1–O1	74.04(17)	O6–Gd2–O8	100.29(19)
O4B–Gd1–O2	80.98(18)	O6–Gd2–O9	72.36(19)
O4B–Gd1–O3	91.45(18)	O7–Gd2–O8	72.16(18)
O4B–Gd1–O4	70.01(17)	O7–Gd2–O9	120.30(17)
O4B–Gd1–O5	137.29(18)	O8A ⁽ⁱⁱⁱ⁾ –Gd2–O7	74.53(18)
O4B–Gd1–O11A ⁽ⁱ⁾	112.44(17)	O8A ⁽ⁱⁱⁱ⁾ –Gd2–O8	79.56(18)
O7A ⁽ⁱⁱ⁾ –Gd1–O1	73.49(18)	O8A ⁽ⁱⁱⁱ⁾ –Gd2–O9	136.30(18)
O7A ⁽ⁱⁱ⁾ –Gd1–O2	80.69(17)	O8–Gd2–O9	68.89(18)
O7A ⁽ⁱⁱ⁾ –Gd1–O3	88.17(18)	O12B ^(iv) –Gd2–O3B	72.37(18)
O7A ⁽ⁱⁱ⁾ –Gd1–O4	143.59(17)	O12B ^(iv) –Gd2–O6	78.39(18)
O7A ⁽ⁱⁱ⁾ –Gd1–O4B	145.94(18)	O12B ^(iv) –Gd2–O7	139.59(18)
O7A ⁽ⁱⁱ⁾ –Gd1–O5	74.33(17)	O12B ^(iv) –Gd2–O8A ⁽ⁱⁱⁱ⁾	123.13(18)
O7A ⁽ⁱⁱ⁾ –Gd1–O11A ⁽ⁱ⁾	87.6(17)	O12B ^(iv) –Gd2–O8	141.49(18)
O11A ⁽ⁱ⁾ –Gd1–O5	70.26(19)	O12B ^(iv) –Gd2–O9	74.27(18)

Symmetry code(s): (i) $-y+1, -x+1, -z+1/2$; (ii) $-y+3/2, x+1/2, z-1/4$; (iii) $-x+1/2, y+1/2, -z+3/4$; (iv) $-x+3/2, y-1/2, -z+3/4$.

Table S4. Selected bond angles ω (deg.) for **1_{Tb}**.

Angle	ω	Angle	ω
O7A–Tb1–O11A ⁽ⁱ⁾	87.25(16)	O3A–Tb2–O8A ⁽ⁱ⁾	73.27(15)
O7A–Tb1–O1	73.37(16)	O3A–Tb2–O3B	74.77(15)
O7A–Tb1–O2	80.88(15)	O3A–Tb2–O12B ⁽ⁱⁱⁱ⁾	112.22(15)
O7A–Tb1–O3	143.72(15)	O3A–Tb2–O6	74.77(15)
O7A–Tb1–O4	88.41(16)	O3A–Tb2–O7	142.30(16)
O7A–Tb1–O5	74.12(15)	O3A–Tb2–O8	142.93(16)
O11A ⁽ⁱ⁾ –Tb1–O4	140.53(17)	O3A–Tb2–O9	84.49(16)
O11A ⁽ⁱ⁾ –Tb1–O5	69.78(17)	O8Ai–Tb2–O6	136.37(15)
O11B ⁽ⁱⁱ⁾ –Tb1–O7A	145.95(15)	O8Ai–Tb2–O8	74.35(16)
O11B ⁽ⁱⁱ⁾ –Tb1–O11A ⁽ⁱ⁾	112.99(16)	O8Ai–Tb2–O9	79.37(15)
O11B ⁽ⁱⁱ⁾ –Tb1–O1	74.13(16)	O3B–Tb2–O8A ⁽ⁱ⁾	123.14(15)
O11B ⁽ⁱⁱ⁾ –Tb1–O2	80.77(15)	O3B–Tb2–O12B ⁽ⁱⁱⁱ⁾	72.76(15)
O11B ⁽ⁱⁱ⁾ –Tb1–O3	69.95(15)	O3B–Tb2–O6	74.55(16)
O11B ⁽ⁱⁱ⁾ –Tb1–O4	91.53(16)	O3B–Tb2–O8	139.83(15)
O11B ⁽ⁱⁱ⁾ –Tb1–O5	137.48(16)	O3B–Tb2–O9	141.39(16)
O1–Tb1–O11A ⁽ⁱ⁾	141.89(15)	O12B ⁽ⁱⁱⁱ⁾ –Tb2–O8A ⁽ⁱ⁾	77.64(15)
O1–Tb1–O4	72.77(16)	O12B ⁽ⁱⁱⁱ⁾ –Tb2–O6	142.94(16)
O1–Tb1–O5	131.49(17)	O12B ⁽ⁱⁱⁱ⁾ –Tb2–O8	77.46(15)
O2–Tb1–O11A ⁽ⁱ⁾	70.53(15)	O12B ⁽ⁱⁱⁱ⁾ –Tb2–O9	145.85(15)
O2–Tb1–O1	74.13(15)	O7–Tb2–O8A ⁽ⁱ⁾	144.40(16)
O2–Tb1–O3	121.78(16)	O7–Tb2–O3B	78.17(15)
O2–Tb1–O4	146.87(16)	O7–Tb2–O12B ⁽ⁱⁱⁱ⁾	83.56(17)

O2–Tb1–O5	133.56(16)	O7–Tb2–O6	73.04(16)
O3–Tb1–O11A ⁽ⁱ⁾	76.36(15)	O7–Tb2–O8	72.20(16)
O3–Tb1–O1	136.56(15)	O7–Tb2–O9	101.40(17)
O3–Tb1–O4	84.47(16)	O8–Tb2–O6	119.92(16)
O3–Tb1–O5	69.88(16)	O8–Tb2–O9	72.21(15)
O4–Tb1–O5	71.30(18)	O9–Tb2–O6	68.68(16)

Symmetry code(s): (i) $x+1/2, -y-1/2, -z-1/4$; (ii) $-y-1, -x-1, -z-1/2$; (iii) $x+1/2, -y-3/2, -z-1/4$.

Table S5. Hydrogen bond parameters in structure **1Eu**.

Fragment D–H···A	Distance/ Å			D–H···A /°
	D–H	H···A	D···A	
O1–H1A···O12A ⁽ⁱ⁾	0.98	1.76	2.729(5)	167
O1–H1B···O2S ⁽ⁱ⁾	0.88	1.79	2.651(5)	168
O2–H2A···O2S ⁽ⁱ⁾	0.98	1.86	2.721(5)	145
O2–H2B···O4B ⁽ⁱⁱ⁾	0.85	1.91	2.741(5)	166
O3–H3A···O5	0.98	2.38	2.787(5)	104
O3–H3A···O9	0.98	2.17	3.151(5)	179
O3–H3B···O6S ⁽ⁱ⁾	0.98	1.68	2.660(5)	180
O4–H4A···O1S	0.98	1.79	2.771(5)	179
O4–H4B···O4S ⁽ⁱ⁾	0.80	1.93	2.719(5)	167
O5–H5A···O5A	0.84	1.94	2.749(4)	162
O5–H5A···O7A	0.84	2.57	2.918(5)	106
O5–H5B···O9	0.86	1.97	2.822(5)	175
O6–H6A···O4S	0.84	1.94	2.749(5)	163
O6–H6A···O7	0.84	2.54	2.887(5)	106
O6–H6B···O1A	0.86	2.09	2.866(4)	151
O7–H7A···O1B	0.98	1.81	2.788(4)	180
O7–H7A···O3B	0.98	2.39	2.989(5)	119
O7–H7B···O3S	0.98	1.65	2.630(6)	179
O8–H8A···O5S	0.84	1.87	2.703(6)	176
O8–H8A···O9	0.84	2.55	2.870(5)	104
O8–H8B···O10B ⁽ⁱⁱⁱ⁾	0.84	1.98	2.751(4)	154
O9–H9A···O5S	0.98	2.54	2.872(6)	100
O9–H9A···O6A ⁽ⁱⁱ⁾	0.98	2.00	2.983(4)	180
O9–H9A···O8A ⁽ⁱⁱ⁾	0.98	2.46	3.095(5)	122
O9–H9B···O8S ⁽ⁱ⁾	0.98	1.96	2.919(12)	164
O9–H9B···O8' ⁽ⁱ⁾	0.98	1.77	2.683(16)	154
O1S–H1SA···O12A	0.89	1.93	2.808(4)	166
O1S–H1SB···O12A	1.15	1.75	2.808(4)	150
O2S–H2SA···O8B ^(iv)	0.98	1.85	2.742(5)	150
O2S–H2SB···O4A ^(v)	0.98	1.95	2.836(5)	149
O3S–H3SA···O2B ⁽ⁱⁱⁱ⁾	0.95	2.02	2.960(6)	170
O3S–H3SA···O4B ⁽ⁱⁱⁱ⁾	0.95	2.50	2.996(6)	113
O3S–H3SB···O7S	0.98	2.49	2.942(8)	108

O3S–H3SB···O10S	0.98	2.47	2.905(8)	106'
O3S–H3SB···O7'	0.98	2.56	3.076(10)	113
O3S–H3SB···O9S ^(vi)	0.98	2.30	3.243(10)	161
O3S–H3SB···O9' ^(vi)	0.98	2.26	3.236(16)	175
O3S–H3SB···O9' ⁽ⁱⁱⁱ⁾	0.98	2.46	2.910(17)	108
O4S–H4SA···O8S	0.80	1.92	2.706(12)	165
O4S–H4SA···O8'	0.80	2.08	2.820(15)	153
O4S–H4SB···O1B	0.80	2.47	3.123(5)	139
O4S–H4SB···O9B	0.80	2.17	2.859(4)	144
O5S–H5SA···O2A ⁽ⁱⁱ⁾	0.98	1.97	2.798(6)	140
O5S–H5SB···O7S ⁽ⁱ⁾	0.95	1.88	2.685(8)	140
O5S–H5SB···O7' ⁽ⁱ⁾	0.95	1.78	2.694(9)	161
O6S–H6SA···O5B	0.98	1.82	2.797(5)	172
O6S–H6SB···O4A ^(vii)	0.98	1.97	2.852(6)	148
O7S–H7SA···O7B	1.09	1.76	2.828(8)	163
O7S–H7SB···O6S	0.95	2.22	3.168(8)	178
O8S–H8SA···O7S	0.87	1.94	2.715(15)	148
O8S–H8SA···O10S	0.87	1.96	2.391(16)	109
O8S–H8SA···O7'	0.87	2.58	3.360(17)	149
O8S–H8SB···O8S ⁽ⁱ⁾	0.87	2.21	3.042(17)	160
O9S–H9SA···O8B	0.98	1.82	2.774(10)	164
O9S–H9SB···O3S ^(viii)	0.95	2.29	3.243(10)	178
O9S–H9SB···O7' ^(viii)	0.95	2.58	2.951(16)	104
O9S–H9SB···O9' ^(ix)	0.95	2.47	2.854(17)	104
C9B–H9BB···O2B ⁽ⁱⁱⁱ⁾	0.99	2.55	3.412(6)	146

Symmetry codes: (i) $1-y, 1-x, 1/2-z$; (ii) $-1/2+x, 1/2-y, 1/4-z$; (iii) $-1/2+x, 3/2-y, 1/4-z$; (iv) $1/2+x, 3/2-y, 1/4-z$; (v) $1/2+x, 1/2-y, 1/4-z$; (vi) $-1/2+y, 3/2-x, 1/4+z$; (vii) $1/2+y, 3/2-x, 1/4+z$; (viii) $3/2-y, 1/2+x, -1/4+z$; (ix) $y, x, -z$.

Table S6. Hydrogen bond parameters in structure **1_{Gd}**.

Fragment D–H···A	Distance/ Å			D–H···A /°
	D–H	H···A	D···A	
O1–H1A···O2	0.87	2.55	2.886(7)	104
O1–H1A···O5S ⁽ⁱ⁾	0.87	1.79	2.659(7)	180
O1–H1B···O12A ⁽ⁱⁱ⁾	0.87	1.91	2.728(7)	156
O2–H2A···O11B ⁽ⁱⁱⁱ⁾	0.98	1.80	2.738(8)	158
O2–H2B···O5S ⁽ⁱ⁾	0.98	1.79	2.729(8)	158
O3–H3A···O6S ⁽ⁱⁱ⁾	0.87	1.79	2.653(8)	173
O3–H3B···O1	0.87	2.50	2.813(7)	102
O3–H3B···O1S ^(iv)	0.87	2.13	2.766(8)	129
O4–H4A···O4B	0.87	2.35	2.734(7)	107
O4–H4A···O4S	0.87	1.90	2.665(8)	147
O4–H4B···O9A ^(v)	0.87	1.92	2.710(6)	150
O5–H5A···O5A ^(iv)	0.87	1.87	2.742(8)	179
O5–H5A···O7A ^(iv)	0.87	2.38	2.909(8)	119

O5–H5B···O8 ^(iv)	0.87	2.26	2.811(8)	122
O6–H6A···O2S	0.87	1.80	2.643(8)	162
O6–H6A···O7	0.87	2.45	2.825(7)	107
O6–H6B···O10B ⁽ⁱ⁾	0.87	2.17	2.789(7)	127
O7–H7A···O3S	0.96	1.82	2.701(9)	150
O7–H7B···O1B	0.79	2.00	2.754(8)	161
O8–H8A···O8S	0.87	1.95	2.805(10)	165
O8–H8B···O3S	0.87	2.16	2.863(8)	138
O8–H8B···O6A ^(vi)	0.87	2.30	2.983(7)	135
O9–H9A···O1A	0.98	2.03	2.861(7)	140
O9–H9B···O6S	0.98	1.81	2.753(8)	160
O1S–H1SA···O12A	0.88	2.14	2.814(7)	133
O1S–H1SB···O12A ^(vii)	0.88	2.14	2.814(7)	133
O2S–H2SA···O7S	0.82	2.16	2.962(10)	166
O2S–H2SA···O8S'	0.82	2.60	2.936(13)	106
O2S–H2SB···O8S'	0.87	2.56	2.936(13)	107
O2S–H2SB···O9S'	0.87	2.15	2.99(3)	163
O3S–H3SA···O2A ^(vi)	0.87	1.95	2.803(8)	166
O3S–H3SA···O6A ^(vi)	0.87	2.47	2.965(8)	117
O3S–H3SB···O5S	0.87	2.41	3.209(8)	152
O3S–H3SB···O7S ^(vii)	0.87	2.23	2.675(9)	112
O4S–H4SA···O2B	0.87	2.57	3.304(8)	143
O4S–H4SA···O6B	0.87	2.13	2.799(7)	134
O4S–H4SB···O4A ^(v)	0.87	2.15	2.839(8)	136
O5S–H5SA···O7B	0.87	1.97	2.743(9)	147
O5S–H5SB···O4A ^(vi)	0.87	2.06	2.847(8)	149
O6S–H6SA···O8S ^(vii)	0.87	2.00	2.727(11)	140
O6S–H6SB···O2B ⁽ⁱ⁾	0.87	2.04	2.879(8)	162
O7S–H7SA···O4S ⁽ⁱ⁾	0.99	2.33	3.164(10)	141
O7S–H7SA···O8B ⁽ⁱ⁾	0.99	2.11	2.765(10)	122
O7S–H7SB···O8B ⁽ⁱ⁾	0.99	2.28	2.765(10)	109
O8S–H8SA···O8S'	0.74	1.90	2.58(2)	151
O8S–H8SB···O7S ^(vii)	0.90	1.87	2.717(15)	158
O9S–H9SA···O11B ^(vii)	0.98	2.04	3.00(2)	163
O9S–H9SB···O7S ^(vii)	0.98	2.18	3.13(2)	162
C10B–H10D···O9B ⁽ⁱⁱ⁾	0.99	2.55	3.412(9)	146

Symmetry codes: (i) $3/2-x, -1/2+y, 3/4-z$; (ii) $3/2-x, 1/2+y, 3/4-z$; (iii) $3/2-y, -1/2+x, -1/4+z$; (iv) $3/2-y, 1/2+x, -1/4+z$; (v) $1-y, 1-x, 1/2-z$; (vi) $1/2-x, 1/2+y, 3/4-z$; (vii) $y, x, 1-z$.

Table S7. Hydrogen bond parameters in structure **1_{Tb}**.

Fragment D–H···A	Distance/ Å			D–H···A /°
	D–H	H···A	D···A	
O1–H1A···O12A ⁽ⁱ⁾	0.98	1.77	2.735(7)	167

O1–H1B···O2S ⁽ⁱ⁾	0.88	1.80	2.667(7)	167
O1S–H1S···O12A	0.81	2.12	2.821(6)	145
O2–H2A···O7 ⁽ⁱⁱ⁾	0.98	1.63	2.56(9)	155
O2–H2A···O2S ⁽ⁱ⁾	0.98	1.85	2.730(7)	147
O2–H2B···O4B ⁽ⁱⁱⁱ⁾	0.86	1.90	2.739(7)	165
O3–H3A···O5	0.98	2.36	2.768(7)	104
O3–H3A···O9	0.98	2.18	3.158(7)	179
O3–H3B···O6S ⁽ⁱ⁾	0.98	1.69	2.673(8)	178
O4–H4A···O1S	0.92	1.86	2.754(7)	164
O4–H4B···O4S ⁽ⁱ⁾	1.04	1.69	2.635(7)	148
O5–H5A···O5A	0.84	1.93	2.742(6)	162
O5–H5A···O7A	0.84	2.56	2.897(7)	105
O5–H5B···O9	0.86	1.97	2.824(7)	176
O6–H6A···O4S	0.84	1.93	2.743(7)	162
O6–H6A···O7	0.84	2.52	2.867(7)	106
O6–H6B···O1A	0.86	2.08	2.870(6)	151
O7–H7A···O1B	0.98	1.80	2.781(7)	179
O7–H7A···O3B	0.98	2.38	2.968(6)	118
O7–H7B···O3S	0.98	1.66	2.640(8)	177
O8–H8A···O5S	0.84	1.88	2.714(8)	176
O8–H8A···O9	0.84	2.53	2.858(7)	104
O8–H8B···O10B ^(iv)	0.83	1.98	2.750(6)	154
O9–H9A···O6A ⁽ⁱⁱⁱ⁾	0.98	1.98	2.954(6)	180
O9–H9A···O8A ⁽ⁱⁱⁱ⁾	0.98	2.45	3.072(6)	121
O9–H9B···O8S ⁽ⁱ⁾	0.98	1.99	2.941(13)	164
O9–H9B···O8 ⁽ⁱ⁾	0.98	1.75	2.668(16)	155
O2S–H2SA···O8B ^(v)	0.98	1.85	2.751(7)	150
O2S–H2SB···O4A ^(vi)	0.98	1.99	2.867(7)	148
O3S–H3SA···O2B ^(iv)	0.95	2.01	2.949(8)	169
O3S–H3SA···O4B ^(iv)	0.95	2.51	3.007(8)	113
O3S–H3SB···O7S	0.98	2.45	2.933(10)	110
O3S–H3SB···O4S'	0.98	2.46	2.907(13)	108
O3S–H3SB···O9S ^(vii)	0.98	2.32	3.260(14)	160
O3S–H3SB···O9 ^(vii)	0.98	2.25	3.23(2)	174
O3S–H3SB···O9 ^(iv)	0.98	2.50	2.95(2)	108
O4S–H4SA···O8S	0.80	1.88	2.665(13)	166
O4S–H4SA···O8'	0.80	2.17	2.902(17)	152
O4S–H4SB···O1B	0.80	2.51	3.162(7)	140
O4S–H4SB···O9B	0.80	2.23	2.925(7)	145
O5S–H5SA···O2A ⁽ⁱⁱⁱ⁾	0.98	1.97	2.803(8)	141
O5S–H5SB···O7S ⁽ⁱ⁾	0.95	1.85	2.689(9)	146
O5S–H5SB···O7 ⁽ⁱ⁾	0.95	2.28	3.16(8)	154
O6S–H6SA···O5B	0.98	1.83	2.807(7)	172
O6S–H6SB···O4A ^(viii)	0.98	1.97	2.854(8)	149

O7S–H7SA···O7B	0.98	1.84	2.773(9)	158
O7S–H7SB···O6S	0.98	2.22	3.199(10)	173
O8S–H8SA···O7S	0.87	2.11	2.892(17)	149
O8S–H8SA···O4S'	0.87	2.00	2.44(2)	110
O8S–H8SB···O8S ⁽ⁱ⁾	0.87	2.22	3.05(2)	159
O9S–H9SA···O8B	0.98	1.82	2.778(14)	165
O9S–H9SB···O3S ^(ix)	0.95	2.31	3.260(14)	178
O9S–H9SB···O9' ^(x)	0.95	2.46	2.86(2)	105
C9B–H9BA···O2B ^(iv)	0.99	2.54	3.414(8)	148

Symmetry codes: (i) $-1-y, -1-x, -1/2-z$; (ii) $x, 1+y, z$; (iii) $1/2+x, -1/2-y, -1/4-z$; (iv) $1/2+x, -3/2-y, -1/4-z$; (v) $-1/2+x, -3/2-y, -1/4-z$; (vi) $-1/2+x, -1/2-y, -1/4-z$; (vii) $1/2+y, -3/2-x, -1/4+z$; (viii) $-1/2+y, -3/2-x, -1/4+z$; (ix) $-3/2-y, -1/2+x, 1/4+z$; (x) $y, x, -z$.

Table S8. Hydrogen bond parameters in structure **3**.

Fragment D–H···A	Distance/ Å			D–H···A /°
	D–H	H···A	D···A	
O1S–H1S'···O10 ⁽ⁱ⁾	0.86	1.97	2.770(3)	154
O1S–H1S···O9 ⁽ⁱⁱ⁾	0.85	1.95	2.798(3)	175
O2S–H2S'···O6 ⁽ⁱⁱⁱ⁾	0.85	2.02	2.869(3)	174
O2S–H2S···O1 ^(iv)	0.89	1.83	2.706(2)	169
O5–H5···O7 ^(v)	0.89	1.88	2.774(3)	175
O5–H5'···O1S	0.87	1.74	2.604(3)	171
O6–H6···O4 ⁽ⁱⁱⁱ⁾	0.83	1.94	2.765(2)	170
O6–H6'···O9 ^(vi)	0.81	1.81	2.605(2)	169
O8–H8···O5 ⁽ⁱ⁾	0.95	2.39	3.341(3)	180

Symmetry codes: (i) $1-x, 1/2+y, 3/2-z$; (ii) $2-x, 1/2+y, 3/2-z$; (iii) $1-x, 1-y, 1-z$; (iv) $-1+x, y, z$; (v) $2-x, -1/2+y, 3/2-z$; (vi) $2-x, 1-y, 1-z$.

III. Magnetic properties

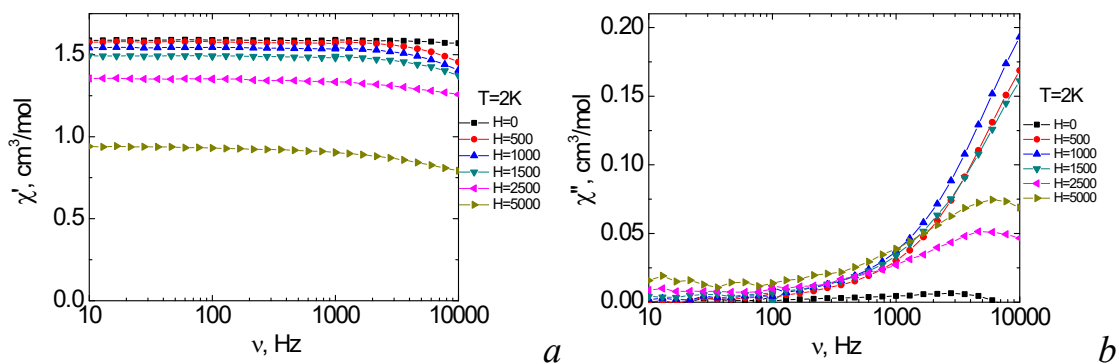


Fig. S10. Frequency dependencies of in-phase, χ' (a) and out-of-phase, χ'' (b) components of dynamic magnetic susceptibility for complex $\mathbf{1}_{Eu}$ at $T = 2$ K under various dc magnetic fields.

Solid lines are visual guides.

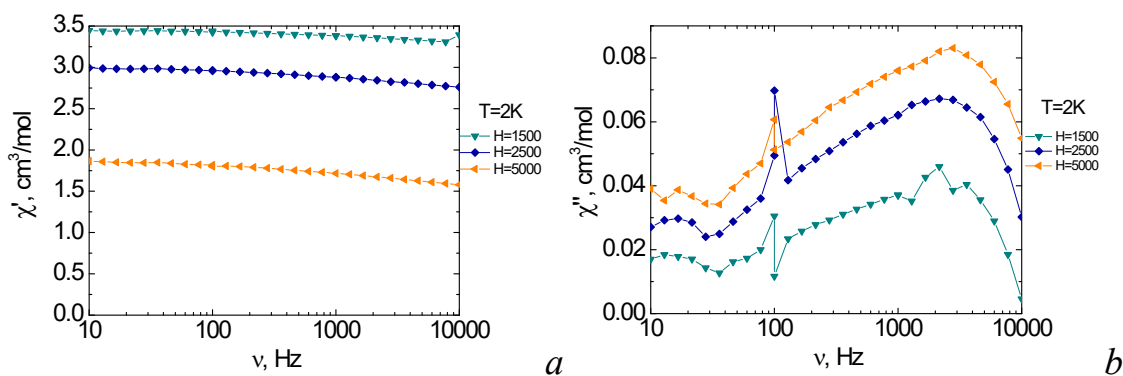


Fig. S11. Frequency dependencies of in-phase, χ' (a) and out-of-phase, χ'' (b) components of dynamic magnetic susceptibility for complex $\mathbf{1}_{Gd}$ at $T = 2$ K under various dc magnetic fields.

Solid lines are visual guides.

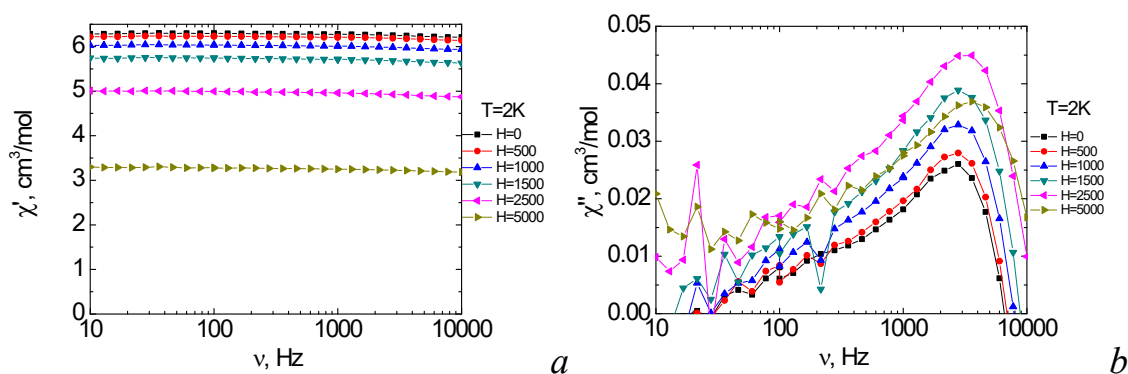


Fig. S12. Frequency dependencies of in-phase, χ' (a) and out-of-phase, χ'' (b) components of dynamic magnetic susceptibility for complex $\mathbf{1}_{Tb}$ at $T = 2$ K under various dc magnetic fields.

Solid lines are visual guides.

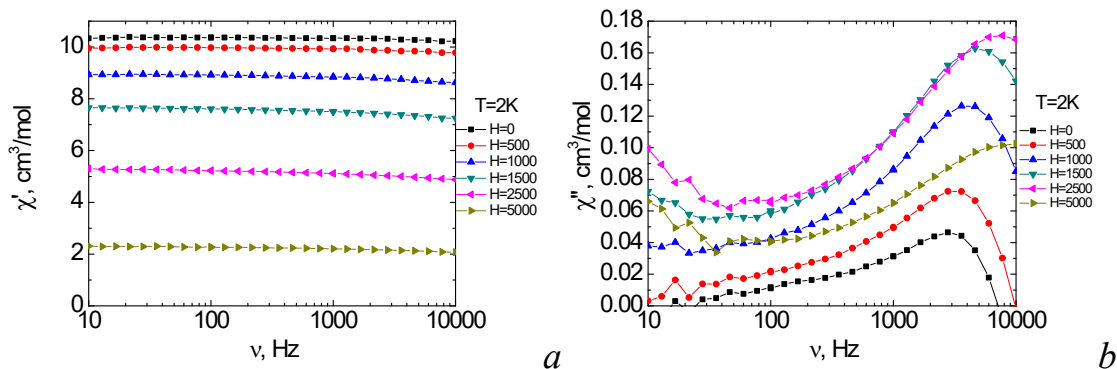


Fig. S13. Frequency dependencies of in-phase, χ' (a) and out-of-phase, χ'' (b) components of dynamic magnetic susceptibility for complex 2_{Dy} at $T = 2$ K under various dc magnetic fields.

Solid lines are visual guides.

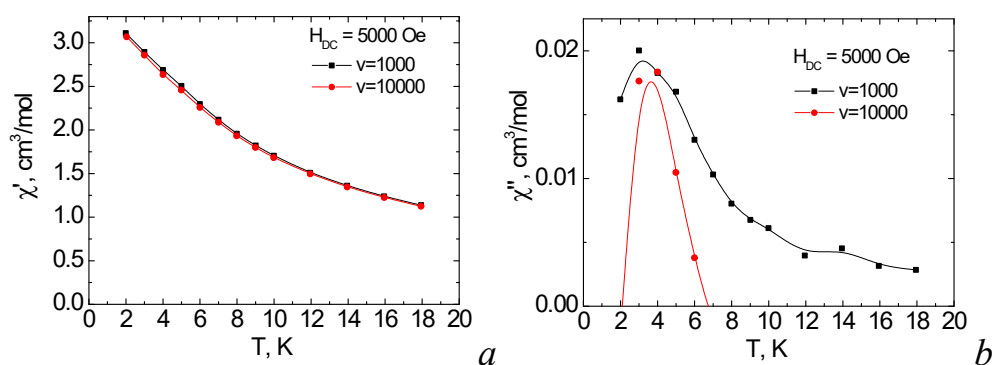


Fig. S14. Frequency dependencies of in-phase, χ' (a) and out-of-phase, χ'' (b) components of dynamic magnetic susceptibility for complex 2_{Ho} under magnetic field $H = 5000$ Oe under various temperatures. Solid lines are visual guides.

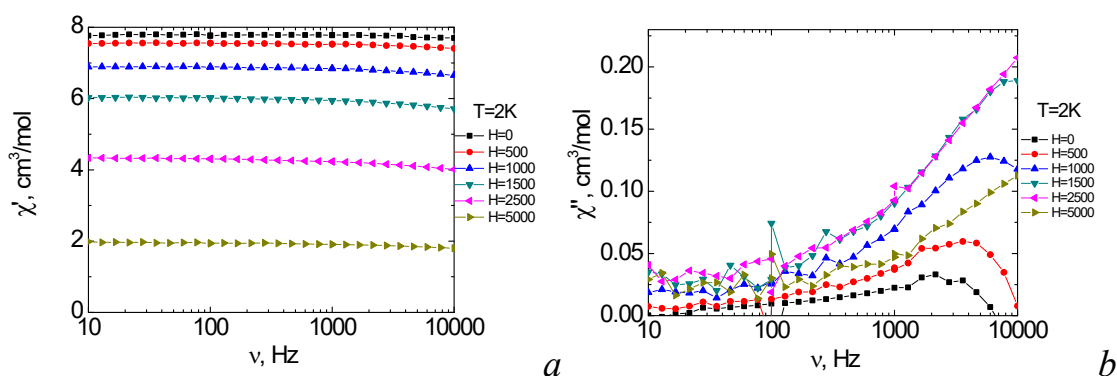


Fig. S15. Frequency dependencies of in-phase, χ' (a) and out-of-phase, χ'' (b) components of dynamic magnetic susceptibility for complex 2_{Er} at $T = 2$ K under various dc magnetic fields.

Solid lines are visual guides.

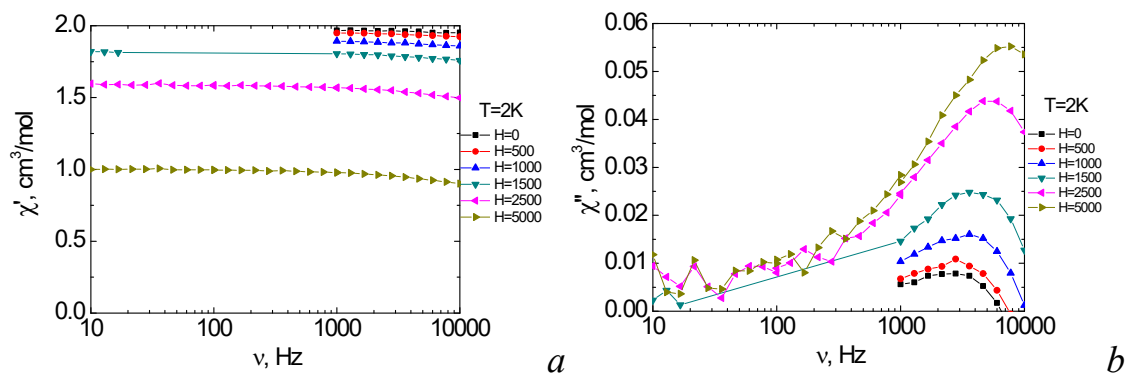


Fig. S16. Frequency dependencies of in-phase, χ' (a) and out-of-phase, χ'' (b) components of dynamic magnetic susceptibility for complex 2_{Vb} at $T = 2$ K under various dc magnetic fields.

Solid lines are visual guides.

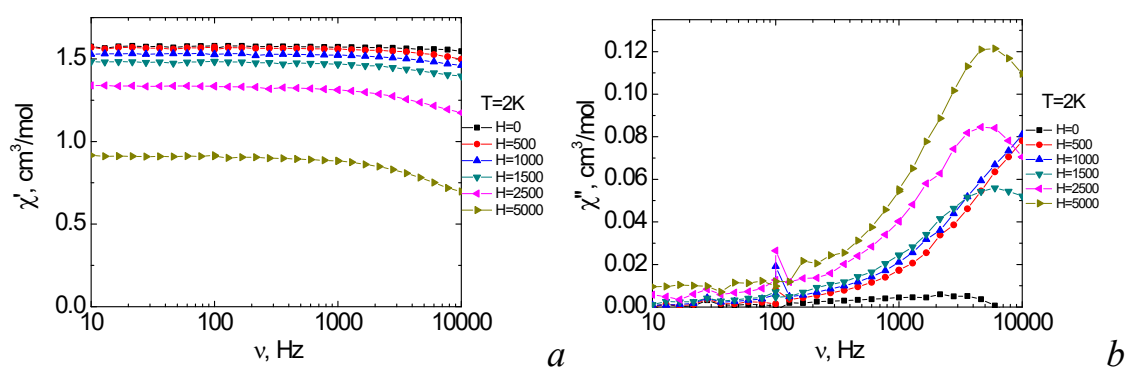


Fig. S17. Frequency dependencies of in-phase, χ' (a) and out-of-phase, χ'' (b) components of dynamic magnetic susceptibility for complex 2_V at $T = 2$ K under various dc magnetic fields.

Solid lines are visual guides.

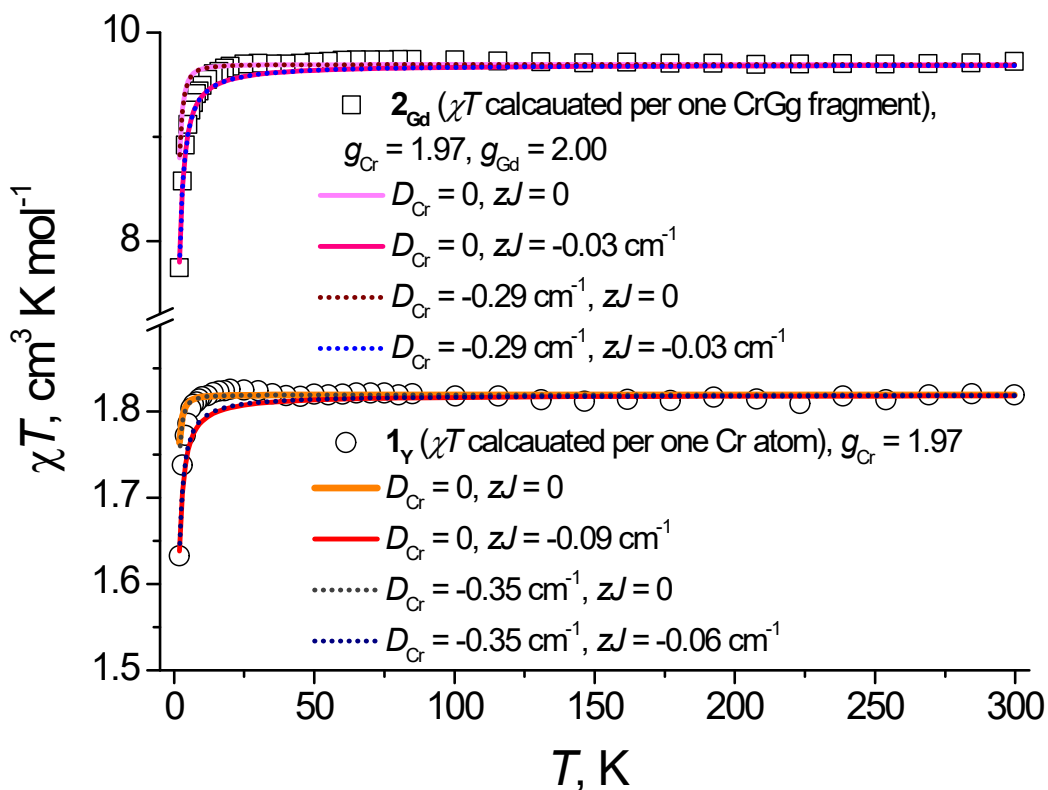


Fig. S18. Experimental χT vs. T plots and fits (see Table S9 for details) for compounds 2_Y (at the bottom) and 1_{Gd} (at the top) at 2-300 K, $H_{dc} = 5000$ Oe.

Table S9. Best-fit approximation parameters of χT vs. T curves for 2_Y and 1_{Gd} (g -factors were fixed: $g_{Cr} = 1.97$, $g_{Gd} = 2.00$; $R^2 = \sum[(\chi_M T)_{exp} - (\chi_M T)_{theor}]^2 / (\sum(\chi_M T)_{exp}^2)$).

Fit number	1	2	3	4
Fit details	$zJ = 0$	$zJ \neq 0$	$zJ = 0$	$zJ \neq 0$
2_Y	$D_{Cr} = 0$		$D_{Cr} = -1.1 \text{ cm}^{-1}$	$D_{Cr} = -0.35 \text{ cm}^{-1}$
	$R^2 = 1.7 \cdot 10^{-4}$	$zJ = -0.09 \text{ cm}^{-1}$, $R^2 = 8.9 \cdot 10^{-5}$	$R^2 = 6.9 \cdot 10^{-5}$	$R^2 = 1.3 \cdot 10^{-4}$, $zJ = -0.06 \text{ cm}^{-1}$, $R^2 = 4.4 \cdot 10^{-5}$
1_{Gd}	$D_{Cr} = 0$		$D_{Cr} = -7.0 \text{ cm}^{-1}$	$D_{Cr} = -0.29 \text{ cm}^{-1}$
	$R^2 = 6.4 \cdot 10^{-4}$	$zJ = -0.03 \text{ cm}^{-1}$, $R^2 = 6.5 \cdot 10^{-5}$	$R^2 = 6.9 \cdot 10^{-5}$	$R^2 = 6.3 \cdot 10^{-4}$, $zJ = -0.03 \text{ cm}^{-1}$, $R^2 = 6.6 \cdot 10^{-5}$

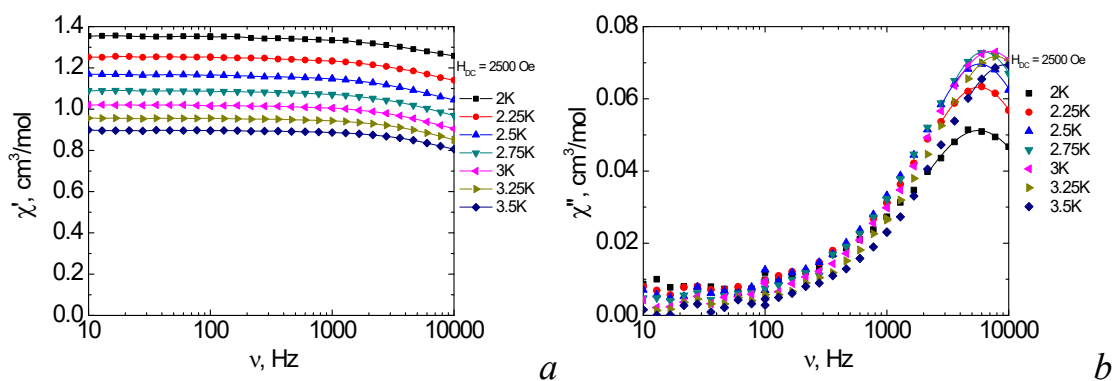


Fig. S19. Frequency dependences of the in-phase χ' (a) and out-of-phase χ'' (b) components of the *ac* magnetic susceptibility between 2 and 3.5 K for 1_{Eu} in 2500 Oe *dc*-field. Solid lines are visual guides (a), fits by the generalized Debye model (b).

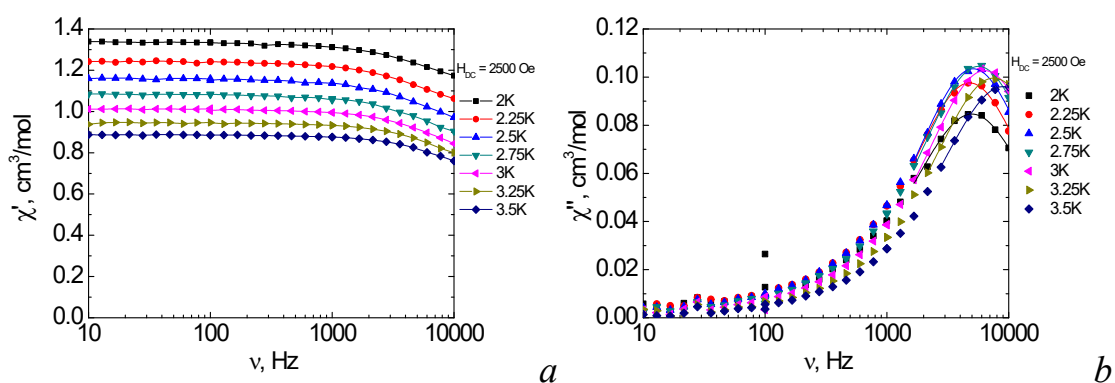


Fig. S20. Frequency dependences of the in-phase χ' (a) and out-of-phase χ'' (b) components of the *ac* magnetic susceptibility between 2 and 3.5 K for 2_{Y} in 2500 Oe *dc*-field. Solid lines are visual guides (a), fits by the generalized Debye model (b).

IV. Quantum-chemical calculations

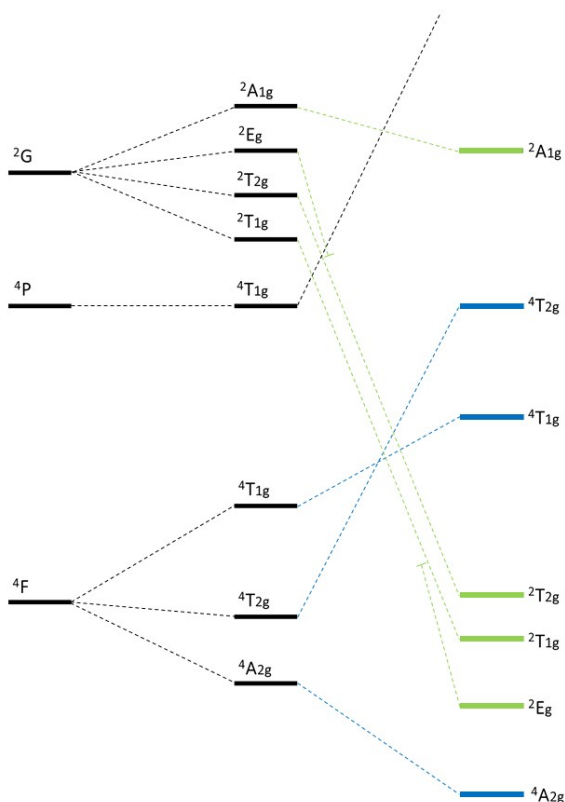


Fig. S21. The scheme of splitting of the three main orbital 4F and 2G levels as a result of distortion of the crystal field (relative arrangement of levels, the scale is not respected).

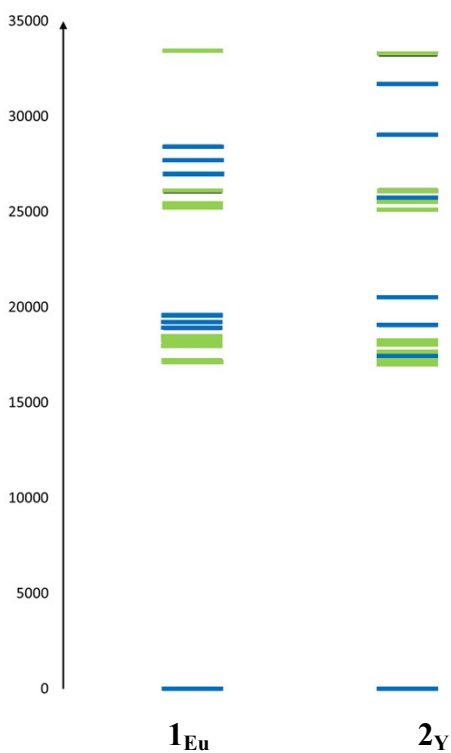


Fig. S22. Calculated energies of components of initial states for complexes 1_{Eu} and 2_Y . Blue and green levels are orbital quartets and doublets, respectively.

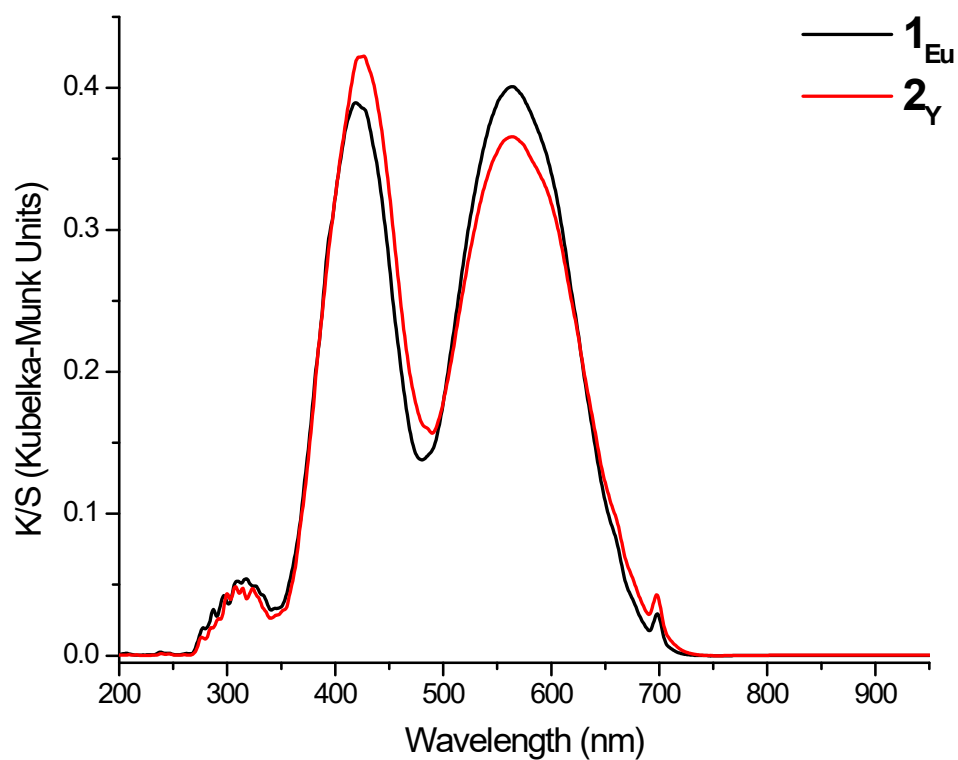


Fig. S23. Diffuse reflectance spectra of compounds 1_{Eu} and 1_Y .

Table S10. Calculated energies of the electronic states for Cr^{3+} ions in complexes 1_{Eu} and 2_Y .

Term	1_{Eu}		2_Y	
	E, cm^{-1}	λ , nm	E, cm^{-1}	λ , nm
$^4A_{2g}$	0	0	0	0
2E_g	17189.0 17214.3	581	17032.8 17085.0	586
$^2T_{1g}$	18024.2 18289.5 18363.1	549	17621.7 18080.3 18246.1	556
$^4T_{1g}$	18904.3 19212.3 19594.4	520	17383.2 19055.7 20518.1	527
$^2T_{2g}$	25229.1 25366.2 26076.6	391	25116.1 25608.7 26130.5	390
$^4T_{2g}$	26991.2 27711.4 28425.5	361	25668.5 29051.5 31691.7	347
$^2A_{1g}$	33446.3	299	33253.1	301

Table S11. The contribution of levels to the axial and rhombic components of magnetic anisotropy.

Term	1_{Eu}		2_Y	
	D	E	D	E
$4T_{1g}$	-0.727	0.135	-1.049	0.099
	0.676	0.188	0.434	-0.608
	-0.055	-0.323	0.379	0.463
$2T_{1g}$	-0.706	-0.711	-0.637	-0.621
	-0.689	0.687	-0.624	0.631
	1.136	-0.002	1.176	-0.025

Table S12. Calculated parameters of spin Hamiltonian (1).

Parameter	1_{Eu}	2_Y
D, cm^{-1}	-0.293	-0.348
E/D	0.098	0.124
g_z	1.970	1.967
g_x	1.972	1.972
g_y	1.971	1.974
g_{iso}	1.971	1.971

Table S13. Energies of six lower Kramers doublets.

1_{Eu}	2_Y
0	0
0.6	0.7
17134.4	16894.4
17170.8	17042.1
17992.1	17360.7
18254.2	17478.8

V. Thermal analysis

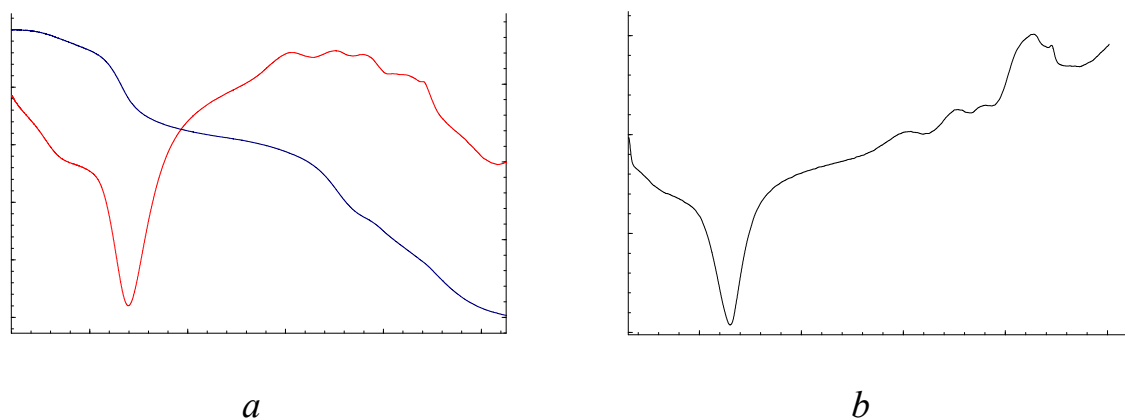


Fig. S24. TGA (blue), DTA (red) (*a*) and DSC (*b*) curves for the thermal decomposition of **1Eu**.

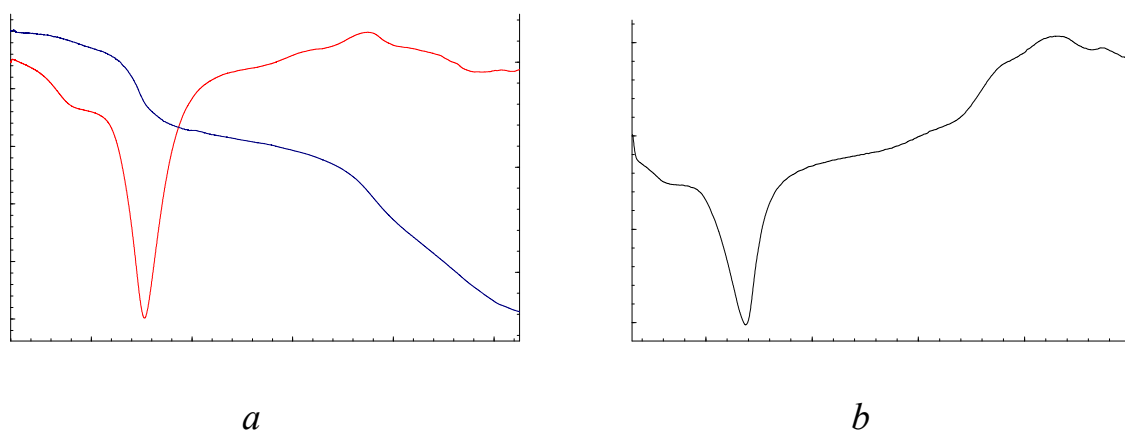


Fig. S25. TGA (blue), DTA (red) (*a*) and DSC (*b*) curves for the thermal decomposition of **1Ga**.

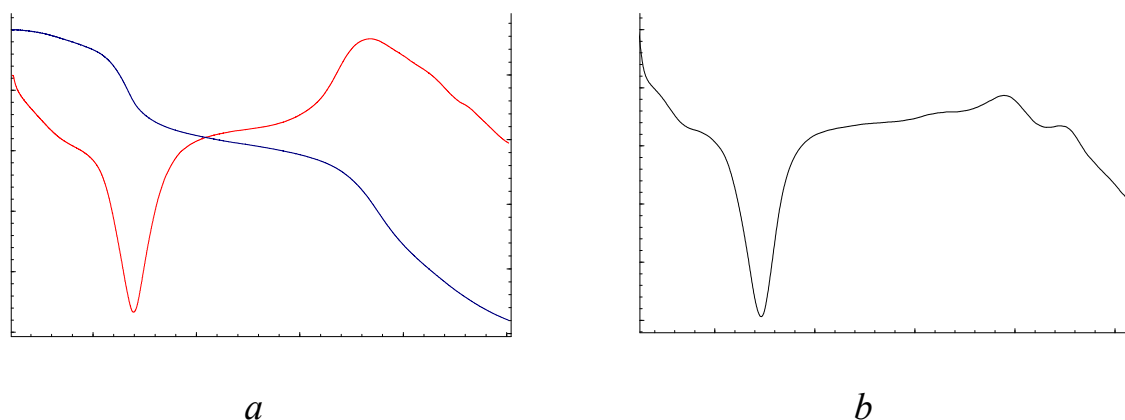


Fig. S26. TGA (blue), DTA (red) (*a*) and DSC (*b*) curves for the thermal decomposition of **1Tb**.

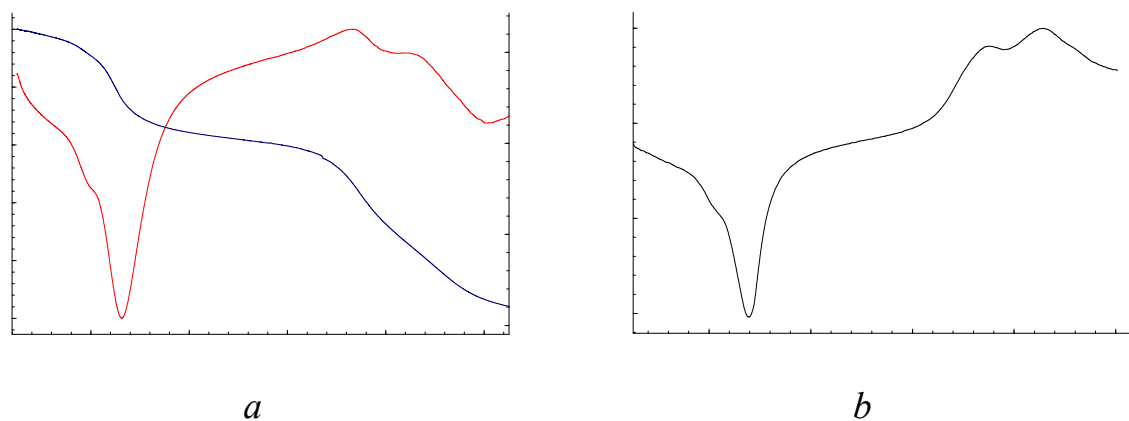


Fig. S27. TGA (blue), DTA (red) (*a*) and DSC (*b*) curves for the thermal decomposition of **2_{Ho}**.

Table S14. Characteristics of the solid-phase thermolysis of **1_{Eu}**, **1_{Gd}**, **1_{Tb}**, **2_{Ho}**.

Complex	t_{onset} (I), °C	t_{onset} (II), °C	t_{onset} (III), °C	Δm (I), %	$\Delta m_{expected}$ (I), %	Δm (II), %	Δm (III), %
1_{Eu}	28	246	534.7	18.9	19.8	30.9	4.8
1_{Gd}	41	283	539.2	19.4	19.7	30.8	6.1
1_{Tb}	25	251	529	19.1	19.6	29.1	4.9
2_{Ho}	26	243.9	541.3	18.9	19.5	29.5	6.2

VI. X-Ray Crystallography

Table S15. Crystallographic parameters and structure refinement statistics for compounds **1_{Eu}**, **1_{Gd}**, **1_{Tb}**, **2_{Ho}**, and **3**.

Parameter	1_{Eu}	1_{Gd}	1_{Tb}	2_{Ho}	3
Empirical formula	C ₃₀ H ₅₉ Cr ₂ Eu ₂ O _{41.5}	C ₃₀ H ₅₉ Cr ₂ Gd ₂ O _{41.5}	C ₃₀ H ₅₉ Cr ₂ Tb ₂ O _{41.5}	C ₃₀ H ₄₈ Cr ₂ Ho ₂ O ₃₇	C ₁₀ H ₁₇ CrO ₁₂
Formula weight (g·mol ⁻¹)	1491.69	1505.61	1502.27	1434.54	381.23
<i>T</i> (K)	150	150	150	150	296
Crystal system	Tetragonal	Tetragonal	Tetragonal	Tetragonal	Monoclinic
Space group	<i>P</i> 4 ₃ 2 ₁ 2	<i>P</i> 4 ₃ 2 ₁ 2	<i>P</i> 4 ₁ 2 ₁ 2	<i>I</i> 4	<i>P</i> 2 ₁ / <i>c</i>
<i>a</i> (Å)	16.2441(3)	16.2257(6)	16.2441(3)	16.2371(6)	8.3636(4)
<i>b</i> (Å)	16.2441(3)	16.2257(6)	16.2441(3)	16.2371(6)	12.1817(6)
<i>c</i> (Å)	38.4605(17)	38.4293(18)	38.4605(17)	20.3655(11)	14.0600(6)
β (deg)	90	90	90	90	97.025(2)
<i>V</i> (Å ³)	10148.6(6)	10117.4(9)	10148.6(6)	5369.2(5)	1421.72(12)
<i>Z</i>	8	8	8	4	4
<i>D</i> _{calc} (g·cm ⁻³)	1.953	1.973	1.971	1.775	1.781
θ _{min} –θ _{max} (deg)	2.38–30.50	2.38–26.39	2.39–30.11	2.51–30.41	2.45–30.48
μ (mm ⁻¹)	2.97	3.12	3.29	3.41	0.87
Crystal size (mm)	0.12×0.11×0.10	0.1×0.05×0.05	0.11×0.11×0.1	0.09×0.08×0.01	0.13×0.11×0.10
Number of measured reflections	105349	50195	84053	20459	7680
Number of independent reflections	13498	9940	9976	5215	2749
Number of reflections with <i>I</i> > 2σ(<i>I</i>)	12821	9054	9384	4997	2464
<i>R</i> _{int}	0.048	0.069	0.059	0.113	0.022
GOOF	1.042	1.037	1.034	1.095	1.208
<i>R</i> _{<i>I</i>} ^[a] , <i>wR</i> ₂ ^[b] (<i>I</i> > 2σ(<i>I</i>))	0.024, 0.056	0.032, 0.064	0.025, 0.055	0.0594, 0.1592	0.035, 0.096
<i>R</i> _{<i>I</i>} ^[a] , <i>wR</i> ₂ ^[b] (all data)	0.027, 0.057	0.039, 0.067	0.029, 0.057	0.0622, 0.1629	0.040, 0.099
<i>T</i> _{min} , <i>T</i> _{max}	0.298, 0.381	0.586, 0.745	0.654, 0.746	0.257, 0.381	0.323, 0.381
Δρ _{max} , Δρ _{min} (e Å ⁻³)	1.9, -0.69	0.69, -0.70	0.70, -0.64	1.72, -1.08	0.50, -0.56

^[a] $R_I = \sum ||F_o| - |F_c|| / \sum |F_o|$. ^[b] $wR_2 = [\sum w(F_o^2 - F_c^2)^2 / \sum w(F_o^2)^2]^{1/2}$